

PŘÍRODOVĚDECKÁ FAKULTA  
UNIVERZITA PALACKÉHO  
OLOMOUC



**BAKALÁŘSKÁ PRÁCE**

2007

Petr Váňa



PŘÍRODOVĚDECKÁ FAKULTA  
UNIVERZITA PALACKÉHO  
OLOMOUC

Katedra Optiky

**Aktivní stabilizace optického výkonu**

BAKALÁŘSKÁ PRÁCE

Autor:	Petr Váňa
Studijní program:	B 1701 Fyzika
Studijní obor:	Optika a Optoelektronika
Forma studia:	prezenční
Vedoucí práce:	Mgr. Miroslav Ježek
Termín odevzdání práce:	.....



**Bibliografická identifikace:**

*Autor:* Petr Váňa

*Název práce:* Active Stabilization of Optical Power

*Typ práce:* Bakalářská práce

*Pracoviště:* Katedra optiky

*Vedoucí práce:* Mgr. Miroslav Ježek

*Rok obhajoby práce:* 2007

*Abstrakt:* Účelem této práce je vyvinout stabilizovaný zdroj optického výkonu. Je diskutován šum ve výkonu spolu s metodou pro porovnání šumů různých optických zdrojů. Zařízení pro stabilizaci je teoreticky navrženo a experimentálně realizováno. Minimální doba odezvy regulace navrženého zařízení je 188 ms. Navržená stabilizace je schopna potlačit nestability ve výkonu v časovém rozsahu jednotek sekund a více. Je popsána a provedena stabilizace několika různých laserových zdrojů. Na závěr je prezentováno možné vylepšení zavedením jednočipového mikropočítače do schématu stabilizace.

*Klíčová slova:* stabilizace, regulace, laser, Allanova variance, šum, optický výkon, Linux, C

*Počet stran:* 28

*Jazyk:* Anglický

**Bibliographical identification:**

*Author:* Petr Váňa

*Title:* Active Stabilization of Optical Power

*Type of thesis:* Bachelor thesis

*Department:* Department of Optics

*Supervisor:* Mgr. Miroslav Ježek

*The year of presentation:* 2007

*Abstract:* The aim of this work is to develop a non-fluctuating optical power source. The power noise is discussed together with an efficient method to compare noises of different sources. The power stabilization device is theoretically designed and experimentally realized. The measured minimum regulation response of the proposed stabilization scheme is 188 ms. The stabilization device can suppress fluctuations in the range of seconds and more. The developed device is applied to different laser sources. Finally, the possible improvement is presented by introducing microcontroller to the design.

*Keywords:* stabilization, regulation, laser, Allan variance, noise, optical power, Linux, C

*Number of pages:* 28

*Language:* English

FACULTY OF NATURAL SCIENCES  
PALACKY UNIVERSITY  
OLOMOUC

Department of Optics

# **Active Stabilization of Optical Power**

Petr Váňa

2007



**Acknowledgment:**

I would like to thank my supervisor Mgr. Miroslav Ježek for his great support and help with solving both the theoretical and the experimental problems. I also thank to RNDr. František Petráš, Zdeněk Weinlich, and Marek Pavlů for both material and knowledge support regarding the electronic circuit design and assembly.

**Statement:**

I thereby claim that I wrote this bachelor work on my own, under supervision of Mgr. Miroslav Ježek, using the resources listed in the reference section. I agree with the use of my work for teaching purposes and for its presentation on the website of the Department of Optics.

Olomouc, 30 May 2007

.....

# Contents

1	Introduction .....	1
2	Theoretical approach .....	2
2.1	Frequency spectrum of noise.....	2
2.2	Time domain characterization of noise.....	3
2.3	Model of stabilization device .....	6
3	Experimental setup .....	11
3.1	Continuous-wave diode laser with fiber output.....	11
3.2	Pulse DPSS laser .....	12
4	Computer implementation .....	13
4.1	Main program function.....	13
4.2	Meter initialization .....	14
4.3	Motor initialization.....	14
4.4	Scan of the regulation dependence .....	14
4.5	Stabilization loop.....	16
5	Stabilization performance.....	20
5.1	Continuous-wave diode laser.....	20
5.2	DPSS laser in pulse regime .....	21
5.3	DPSS laser in pulse regime with temperature variations .....	22
6	Possible improvement .....	23
7	Conclusion.....	24

# 1 Introduction

Laser beams are used in various measuring, information, and industrial applications. It is often required that the intensity and thus optical power of the beam remains unchanged in time. But the perfectly stable optical source does not exist.

There are various factors that add noise to the optical signal. Some of these factors depend on the laser signal generation. The low frequency noise is often caused by a temperature dependence of the laser generation. It is interesting, that even spatial fluctuation of the beam caused by instabilities of optical components contributes to optical power fluctuations.

We ideally want to suppress the noise in the whole frequency spectrum. This is technically impossible due to a finite response time of the stabilization device. Therefore, we need to make a compromise between stabilization speed and an additional noise that the stabilization adds by compensating the fluctuations faster than its own response time. In the result, the stabilization always reduces the noise with frequencies lower than its own response frequency, but adds additional noise to the frequencies higher and even comparable to its response frequency.

The feasible way how to control a stabilization procedure to the experimental device is to use a personal computer or a microchip as a regulation controller. It is also advantageous to regulate the optical signal after it leaves the laser source. This will make the procedure independent on the design of the particular laser source.

The proposed stabilization scheme is used to stabilize laser signal in various physical experiments. The demands are to provide a stable optical source in the range of tens of seconds and more. Examples of applications can be found in [8] and [9].

The theoretical analysis in Chapter 2 discusses various attributes of noise and the theoretical design of stabilization device. The experimental setup is presented in Chapter 3. Chapter 4 explains the computer algorithm controlling the stabilization device. In Chapter 5 the stabilization is applied to different optical outputs and the results are discussed. Finally, a possible improvement of the device is proposed in Chapter 6.

## 2 Theoretical approach

Purpose of this chapter is to describe a noisy laser power output and to develop a method to compare a noise for different laser sources. The power output is generally random time-dependent signal with complex properties. We begin with characterizing the noise in the frequency spectra and then we will try to mathematically evaluate the amount of noise in the system. Finally, the theoretical model of stabilization device will be presented.

### 2.1 Frequency spectrum of noise

The frequency spectrum represents an important quality of noisy signal. We can characterize particular types of noise according to their frequency behavior. Important noise is the white noise which is characterized by the flat spectral power density. The noises whose intensity spectrum follows the

$$\frac{1}{f^a} \quad (1)$$

dependence with  $a$  as the parameter are also significant. Some of them are also known as flickering noise ( $1/f$ ) and random-walk noise ( $1/f^2$ ). In a long period of time the non-stationary drift is the most significant contribution to the source noise. Different types of noise spectral power density are plotted in Fig.1.

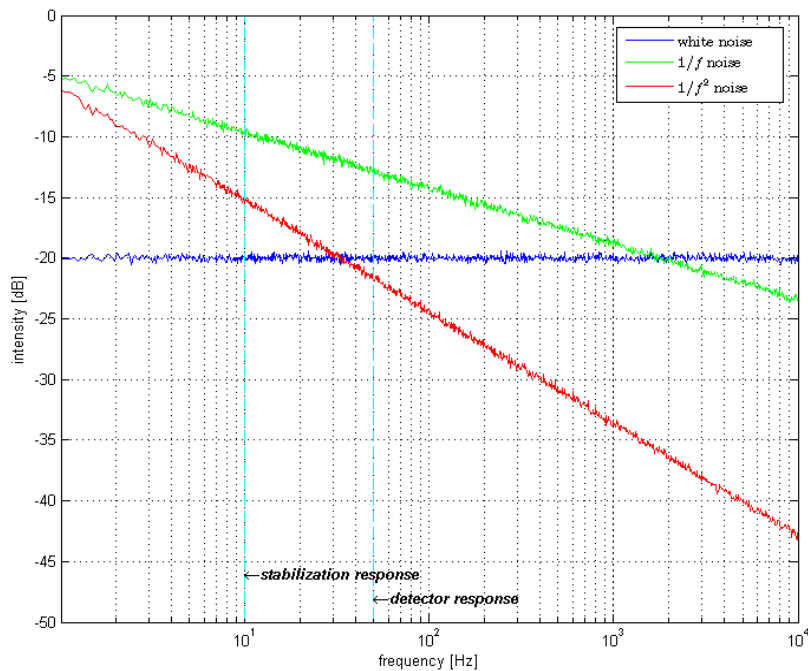


Figure 1: Example of noise spectra. The 10Hz value of stabilization response and 50Hz value of detector response are chosen only for demonstration purposes.

When considering stabilization of any signal we must keep in mind that it is technically impossible to stabilize the source in the whole spectrum. This is due to the finite response time of the stabilization device or the used detector as can be seen in Fig.1. Actually, the signal acquisition response (detector response) and the stabilization response are generally different. Thus the stabilization device can detect fluctuations that cannot be stabilized. The difference between stabilization response and regulation response could cause serious problem in real stabilization scheme which leads to resonant oscillations in the stabilized output. Fortunately, it can be compensated by the regulation algorithm.

## 2.2 Time domain characterization of noise

An example of an output power time evolution of a typical unstabilized laser is shown in Fig.2. The evaluation of the power time evolution is needed to determine how much noise is in the source and eventually how much the applied stabilization device improves the stability of the source. To compare different stabilization approaches we need a mathematical description with simple results.

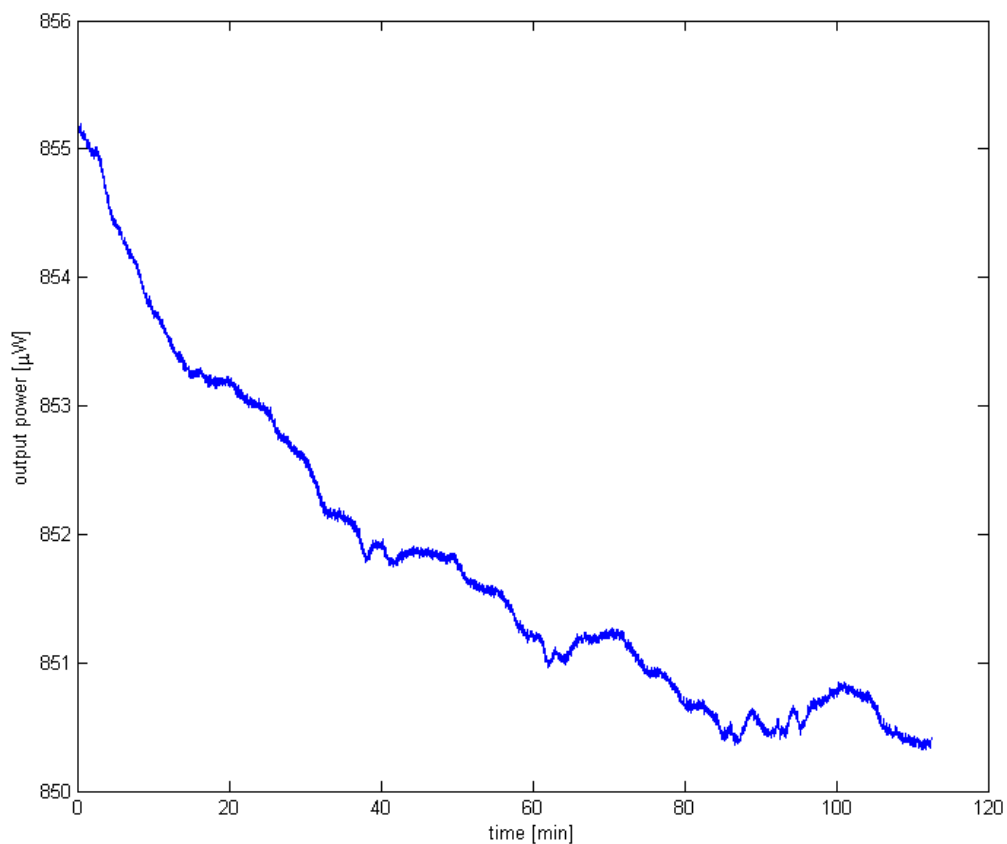


Figure 2: Unstabilized laser power output. The sampling is 1 sample/s. Output is measured

directly from laser with no optical components in the way. The power drift is approximately 0.5% per hour.

To describe fluctuations of the measured power we use following properties.

### **Standard deviation**

The standard deviation, defined as

$$\Delta_{std} = \sqrt{\frac{\sum_{i=1}^n (P_i - \bar{P})^2}{n-1}}, \quad (2)$$

where  $n$  is the number of samples,  $P_i$  is the power value of  $i$ -th sample and  $\bar{P}$  is the mean power of whole set, gives us some basic understanding of the power output fluctuations. However, the deviation defined as (2) does not provide us with the time characteristics of the fluctuations. For example, take the standard deviation of the two sine waves with different frequencies. The standard deviations of both waves are equal, but the waves aren't the same. Thus we may choose a floating window in which we compute the standard deviation. Therefore, we divide the measured dependence into windows. For each window we compute the standard deviation and as a result we take the mean value of these standard deviations. This results in the definition of deviation as

$$\Delta_{k,abs} = \frac{\sum_{j=1}^{\frac{n}{k}} \sqrt{\frac{\sum_{i=1+(j-1) \cdot k}^{j \cdot k} (P_i - \bar{P}_j)^2}{k-1}}}{n}, \quad (3)$$

where  $n$  is the number of samples,  $k$  is the size of window,  $P_i$  is the power value of  $i$ -th sample and  $\bar{P}_j$  is the mean value of power in the  $j$ -th window. Different sources will be compared, so the deviation in (3) must be taken relatively, that means

$$\Delta_{k,rel} = \frac{\Delta_{k,abs}}{\bar{P}}, \quad (4)$$

where  $\bar{P}$  is the mean power value of the whole measured ensemble.

For the measured power output shown in Fig.2 the equation (4) gives the value of  $\Delta_{10,rel} = 2.1 \times 10^{-5}$  or  $\Delta_{60,rel} = 3.4 \times 10^{-5}$  for floating window set to 10 samples (seconds) or 60 samples (seconds), respectively.

There arises a problem what is the best window size to choose. Fortunately, there is a better method designed for characterizing noise and stability in clock systems, called Allan variance and it could be easily adapted for any other type of time evolving quality we are inter-

ested in.

### **Allan Variance**

The Allan variance (AVAR) is a method of analyzing a time sequence to pull out the intrinsic noise in the system as a function of the averaging time. The equation for the two sample variance may be written as follows

$$\sigma_{P,abs}^2(\tau) = \frac{1}{2} \cdot \frac{\sum_{i=1}^{n-1} (P(\tau)_{i+1} - P(\tau)_i)^2}{n-1}, \quad (5)$$

where  $P(\tau)_i$  is the power mean value of the  $i$ -th window.

We explain the idea of the AVAR in the following way: The long time sequence of data is divided into windows, based on an averaging time  $\tau$ . The data in each window are averaged. Then the difference in average between successive windows is squared. Now we have  $n-1$  values, where  $n$  is the number of windows. We average this set of values, divide it by two and as a result we get an Allan variance. This can be done for various averaging time  $\tau$ . The coefficient  $1/2$  adjusts Allan variance to the same dimensions as a classical variance.

We need to compare different sources, therefore we can take the AVAR relatively to the mean power

$$\sigma_{P,rel}(\tau) = \frac{\sigma_{P,abs}(\tau)}{P}. \quad (6)$$

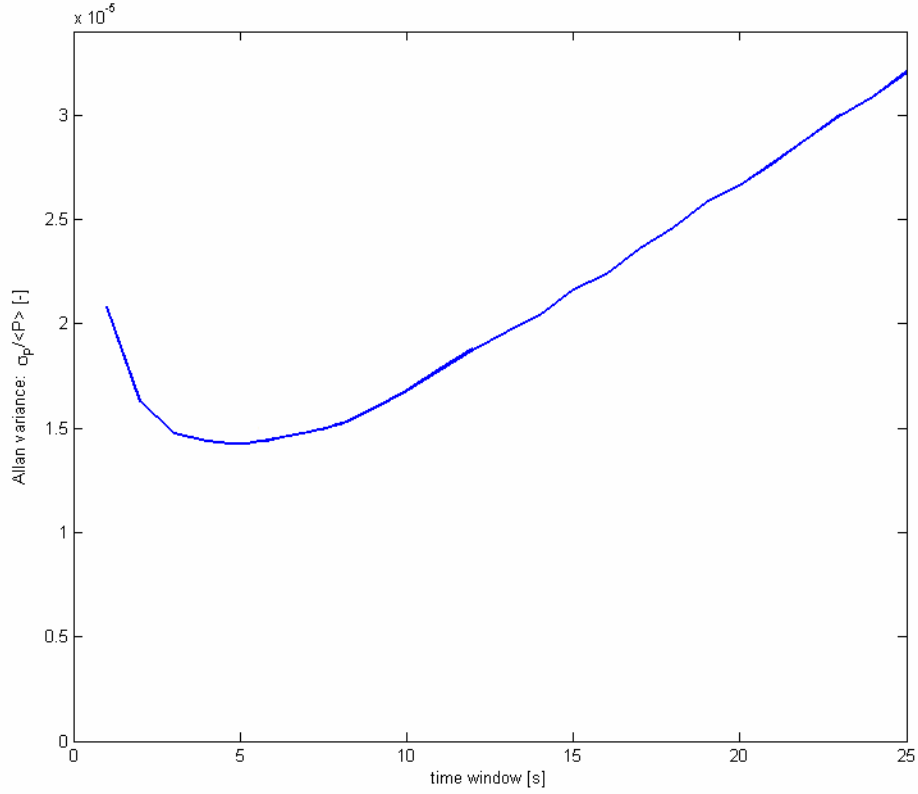


Figure 3: Allan variance of the time sequence of output power plotted in Fig.1. The variance reaches its minimum  $\sigma_{P,rel}(\tau)=1.4 \times 10^{-5}$  for  $\tau = 5$  s.

It can be seen from Fig.3 that the AVAR of unstabilized source reveals the minimum variance for a certain window size. At short averaging times the high-frequency white noise dominates in the sensor and in the source. The variance decreases while averaging over longer times. For a certain averaging time the drift noise of the source prevails and the variance starts to increase. The more detailed explanation can be found in [2].

Both the minimum AVAR value  $\sigma_{P,min}$  and the size of the time window  $\tau_{min}$  corresponding to this minimum describe the source precisely. The time window corresponding to the minimum variance can be interpreted as a time period of a greatest stability of the source (it represents average time of the smallest power deviation). The value of the AVAR describes the magnitude of fluctuations. This provides us a good tool for evaluating and comparing different sources and stabilization approaches.

### 2.3 Model of stabilization device

The effort is to stabilize any optical source. Therefore the stabilization design must be in-

dependent on the laser beam generation. We will apply the stabilization to the laser beam using optical components right after the beam leaves the laser. To achieve this we will use a simple feedback stabilization technique that can be seen in Fig.4.

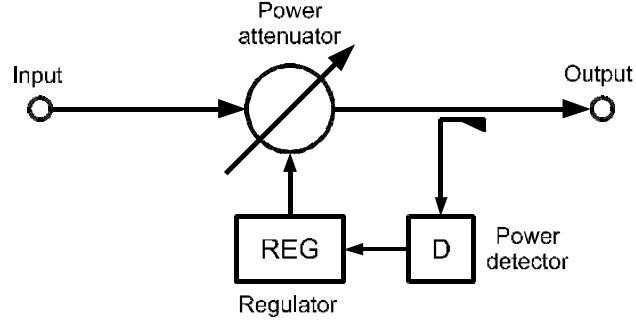


Figure 4: Schematic design of feedback noise-reduction.

We deal with the optical beam thus we need an optical power attenuator. Optical power attenuation can be feasible realized by means of polarization filtering.

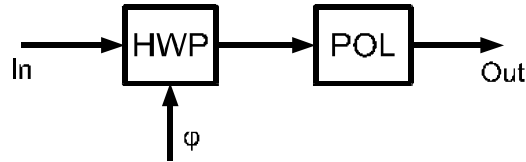


Figure 5: Realization of power attenuation by means of polarization filtering. The angle  $\varphi$  of halfwave plate rotation represents the actuation parameter.

The scheme of polarization attenuation can be seen in Fig. 5. The polarization of incoming beam can be characterized by Jones vector [4]

$$M_{in} = \begin{pmatrix} I_a \\ I_b \end{pmatrix}. \quad (7)$$

The beam then propagates through a rotated half-wave plate. The half-wave plate can be characterized by

$$M_{HWP} = \begin{pmatrix} 1 & 0 \\ 0 & -1 \end{pmatrix} \quad (8)$$

matrix in Jones calculus. The half-wave plate is rotated by angle  $\varphi$  which serves as an actuation parameter. The rotation can be described by a matrix

$$M_{rot} = \begin{pmatrix} \cos \varphi & -\sin \varphi \\ \sin \varphi & \cos \varphi \end{pmatrix}. \quad (9)$$

By passing through the rotated HWP the polarization of the beam is changed. In the case of the linearly polarized incoming beam, the plane of the polarization is simply rotated. The output beam with rotated polarization then passes through a linear polarizer with fixed orienta-

tion. The polarizator can be characterized by a matrix

$$M_{POL} = \begin{pmatrix} \cos^2 \theta & \sin \theta \cos \theta \\ \sin \theta \cos \theta & \sin^2 \theta \end{pmatrix}, \quad (10)$$

where  $\theta$  is the angle of the fixed linear polarization. The outgoing beam can be then characterized as

$$M_{Out} = \begin{pmatrix} O_a \\ O_b \end{pmatrix}. \quad (11)$$

With Jones matrices defined for all optical components we can evaluate the polarization of the outgoing beam matrix using equation

$$M_{Out} = M_{POL} \cdot M_{rot}^{-1} \cdot M_{HWP} \cdot M_{rot} \cdot M_{In}. \quad (12)$$

In the realized setup the incoming beam is polarized vertically and the polarizator POL is also set to vertical polarization which yields the parameters

$$I_a = 0, \quad I_b = 1, \quad \theta = \frac{\pi}{2} \quad (13)$$

and the output polarization state given by equation (12) yields

$$M_{Out} = \begin{pmatrix} 0 \\ -\cos 2\varphi \end{pmatrix}. \quad (14)$$

The power transmittance of the polarization attenuator is then defined as

$$\frac{P_{Out}}{P_{In}} = \frac{I_{Out}}{I_{In}} = \frac{O_a^2 + O_b^2}{I_a^2 + I_b^2} = \cos^2 2\varphi. \quad (15)$$

By varying the rotation angle  $\varphi$  of HWP the incoming optical power can be attenuated. The relation (15) can also be measured and the measurement result shown in Fig.6 corresponds to the theoretical prediction.

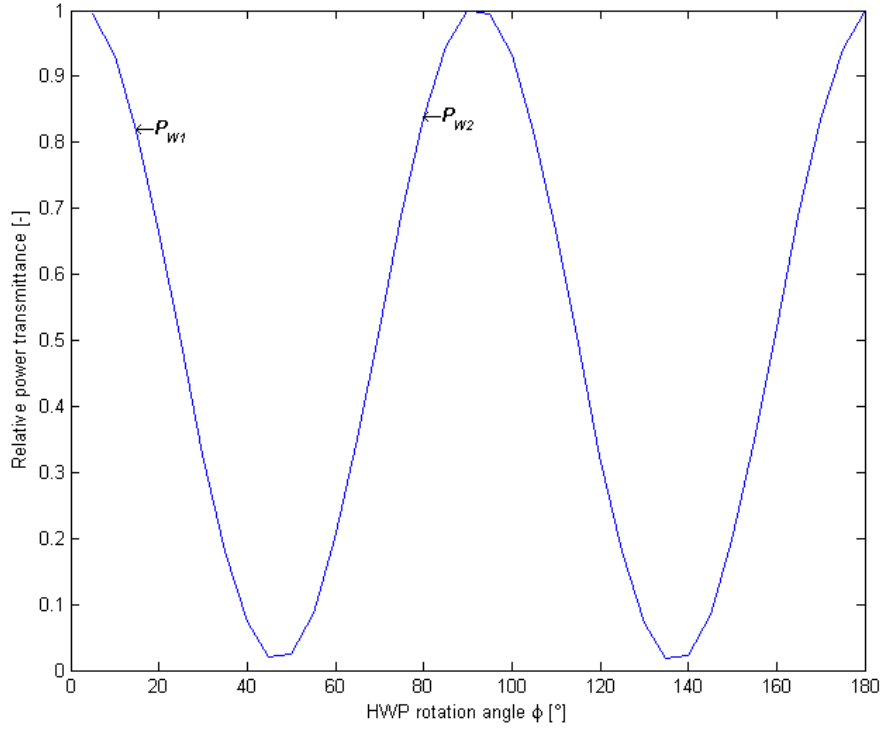


Figure 6: Measured dependence of power transmittance on HWP rotation angle. There are also two possible working points marked.

The power attenuator is controlled by regulator which sets the initial working point of the attenuator (from now on, the reference to working angle means the angle of working point and the reference to working power means the power of working point). The regulator determines the working point in such way that the device is able react to both power increase and decrease. The value of working power depends on particular stabilization requirements. It can be seen from Fig.6 that the working angle choice will result in different attenuation dependence. In the case of the working point  $P_{W1}$  the attenuation raises with decrease of the rotation angle  $\varphi$  but in the case of the working point  $P_{W2}$  the attenuation raises with increase of the rotation angle  $\varphi$ . This must be considered when designing the stabilization algorithm.

We will use a digital computer as a regulator and the attenuation dependence on Fig.6 must be scanned to the computer. Scanning can be done by measuring a few points in the attenuation dependence and then fitting the equation (15) into the data.

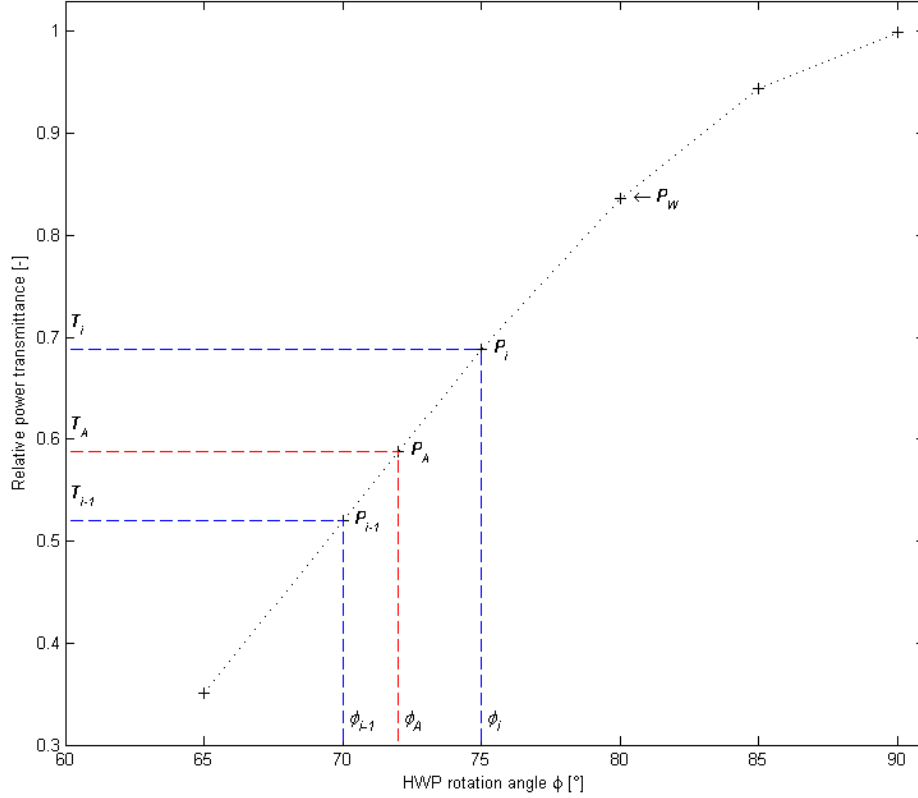


Figure 7: Example of linear interpolation in the digitalized attenuation dependence. The  $P_w$  is the working point,  $P_i$  and  $P_{i-1}$  are the successive points in the scanned dependence.  $P_A$  is the required interpolated point.  $T$  and  $\varphi$  are the transmittance and rotation angle for the given point, respectively.

There is also a second solution closer to the digital nature of the regulator. The attenuation dependence can be scanned by computer. After placing the working point, the computer can scan proximity of the working angle in predefined range by constant angle steps. However, the regulator should evaluate the response angle exactly for the accurate response to the attenuator. Therefore we can linearly interpolate the values between adjacent points in the scanned region. The scheme of linear interpolation can be seen in Fig.7 and it is given by equation

$$\varphi_A = \varphi_i - (P_i - P_A) \cdot \frac{\varphi_i - \varphi_{i-1}}{P_i - P_{i-1}}. \quad (16)$$

### 3 Experimental setup

Our approach is suitable for stabilizing any laser source. The intensity and thus power of the laser beam is regulated in the free space. Therefore the input to the regulator must be adjusted according to type of the stabilized laser.

#### 3.1 Continuous-wave diode laser with fiber output

The diode laser FOSS-01-3S-5/125-810-S-1 (OZ OPTICS) with fiber output emitting near infrared beam with typically  $800\mu\text{W}$  power at wavelength of  $813\text{nm}$ . For the layout of the setup see Fig.8. As was said before, the regulation proceeds after the beam leaves the laser cavity. This laser has a fiber output, therefore we need to collimate the guided beam to free space. The single-mode fiber (SMF) is used to guide the beam to collimator (output coupler). The beam at laser output is linearly polarized but the guidance through a single-mode fiber changes polarization, and we need the regulated beam to be polarized vertically. Therefore the polarization controller is inserted. For proper adjusting of the incoming beam polarization we insert a horizontally set polarizator into the way of the incoming beam and we measure the beam intensity behind the polarizator. Then we adjust the polarization controller. The polarization of the incoming beam is vertical, when the measured intensity is minimal. In our case we measured minimum intensity  $0.511\mu\text{W}$  and maximum intensity  $51.9\mu\text{W}$  with background noise  $(169 \pm 2)\text{ nW}$ . This results in visibility  $98.7\%$  which is sufficient for our purpose.

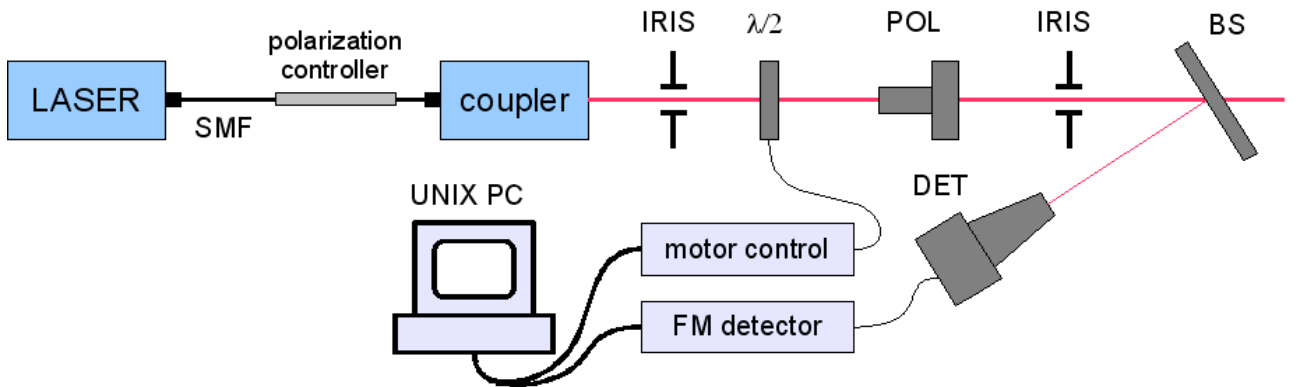


Figure 8: Scheme of stabilization setup in the case of diode laser.

The vertically polarized beam then passes through the iris diaphragm. Diaphragms are useful for verifying the beam position during the setup augments. The combination of motor controlled half-wave plate (HWP) and the polarizator POL represents the regulation actuator. We used a  $800\text{ nm}$  HWP mounted in a SR50CC rotation (Newport). The rotation is controlled by SMC100CC driver (Newport). After passing through the rotated HWP, the beam propagates

through calibrated polarizator POL fixed to vertical polarization. The intensity of the outgoing beam is then splitted by beam splitter BS. The used beam splitter (BS) is the 3mm fused silica plate tilted by a small angle from the perpendicular direction of the outgoing beam. Because the reflection occurs on both plate surfaces, approximately 6% of the beam power is reflected to the detector (DET). As the detector we used a FieldMaster GS power meter with 50mW LM-2 silicon detection head (Coherent). Control of the FieldMaster detector and SMC100CC driver is done by a personal computer.

### 3.2 Pulse DPSS laser

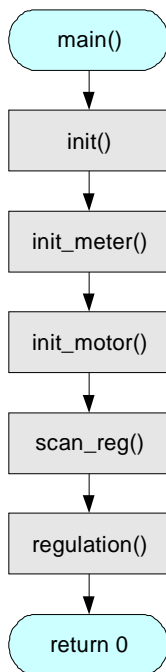
We used the DPSS (diode pumped solid-state) titanium-sapphire laser MIRA 900 (Coherent). This laser can work in CW (continuous-wave) as well as in pulse regime. In pulse regime it provides femtosecond pulses which are tunable from 700 nm to 980 nm with repetition rate of 76 MHz. MIRA laser is pumped by Verdi V-8 CW solid state diode-pumped laser that emits light at wavelength of 532 nm. The beam from MIRA laser can reach average power up to 1 W and peak power of generated pulses up to several thousands of kilo watts. The wavelength used for stabilization experiment was 800 nm.

The MIRA output is a free space propagating beam. We guide the beam from MIRA to about 5 meters distant stabilization setup located at another table. Thus the beam is coupled into the single-mode fiber HP780 (Nufern) and guided to the collimator in the stabilization setup. The 800 mW MIRA power output is reduced by polarization attenuator to the 10 mW which represents the fiber coupler input power  $P_{in}$ . The adjustment of the coupling setup results in the output power  $P_{out} = 6.3 \text{ mW}$  entering the stabilization device. The coupling efficiency given by  $\eta = P_{out} / P_{in}$  is then 63%. The coupling efficiency should be theoretically increased to 85%. For purposes of testing the stabilization device, the coupling efficiency is not a crucial parameter and further improvement is unnecessary. For additional explanation of MIRA laser beam coupling see [3].

## 4 Computer implementation

Both a sensor and a regulation device are controlled by the personal computer with Linux operating system. The stabilization program is written in ANSI C programming language and compiled by GNU C compiler (gcc 3.4.6). The program has two input/output data ports, these are the power meter (FieldMaster GS with 50mW LM-2 silicon detection head), further referred as meter, and the motor controller (Newport SMC100CC), further referred as motor. By reading the measured power value the program evaluates a proper response, which is send to the motor. Both communication lines with the motor and the meter are provided by RS-232 interface, therefore, we used a Linux core libraries *ioctl.h* and *termios.h*. Compared to more common technique of using standard C I/O functions `scanf()` and `printf()` this gives a better control over the port hardware and data transmission. The program is designed to output the measured power and a response to the screen and to a file for developing purposes. For understanding the program function, more detailed description of the important functions follows.

### 4.1 Main program function

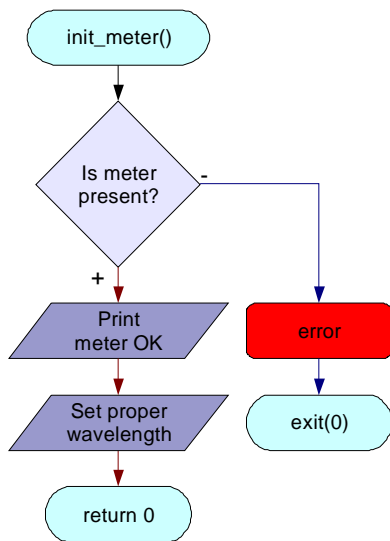


Because the program is written in C language, the `main()` function is called right after the program is executed. The initialization is done by function `init()` that disables the line-buffering on standard output (this has to be done because of the progress bar functioning properly) and prints the welcome message.

Functions `init_meter()` and `init_motor()` prepare the meter and motor devices for operation. Function `scan_reg` retrieves the regulation dependence and sets the motor device to the working point. The function `regulation()` performs the desired stabilization. All these functions are described in further details in next paragraphs.

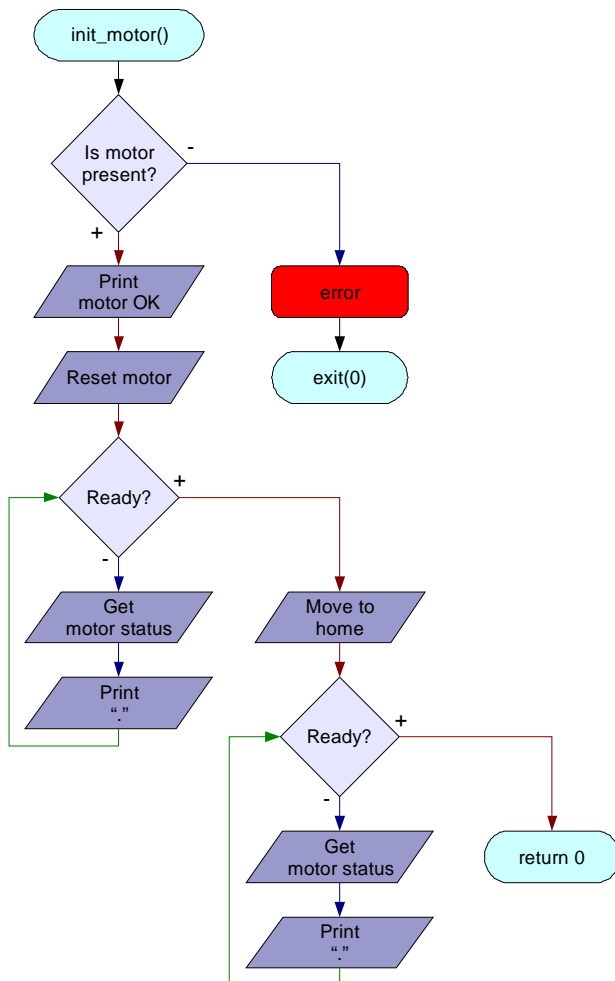
In this program the `main()` function does never return a value (because the regulation proceeds in an infinite loop), so the program termination can be done by the SIGINT system call (CTRL+C).

## 4.2 Meter initialization



Measurement device initialization begins with testing the meter presence. Request to send identification string is sent via serial port to meter, then the serial input is read and received string is compared with the one written in program. If the strings differ, then the message is written to standard error output (on screen) and the program is terminated. Otherwise, program writes confirmation message that meter is found and finally it sets the meter sensitivity to proper wavelength.

## 4.3 Motor initialization

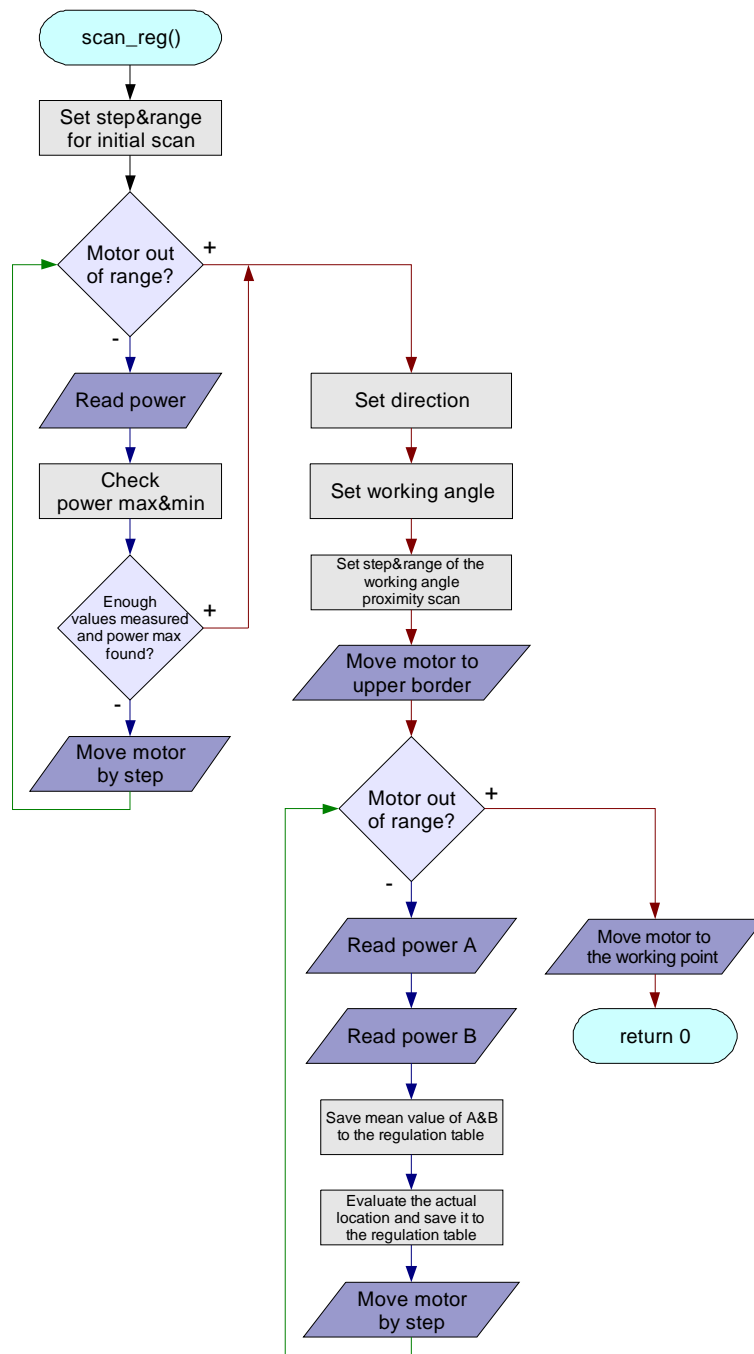


Motor initialization begins by testing the motor presence in the same way as the meter presence was tested.

When it is confirmed that the motor is present, the RESET command is sent to the driver. In the following loop program sends a status request to driver, reads the received status string and compares it with the "ready from RESET" string. If they differ the program writes dot on the screen progress bar and waits a constant time.

Eventually the strings finally match and the homing command is sent, setting the motor to initial position. The waiting loop works just as the previous one. As the motor is set to HOME, the function ends with return 0.

## 4.4 Scan of the regulation dependence



Initially, the matrix for storing the measured power on angle dependence is created, also with the *range* and *step* variables. The maximum range is set to one step more than 90 degrees, because we are using the  $\lambda/2$  plate as regulator, and in this range we will surely find both maximum and minimum transmittance (Fig.6). In order to proceed fast, the big steps are used. In our case the big step was 5 degrees.

The first scanning loop scans the dependence to determine the optimal working point placement. It starts by reading the power value at the initial angle, then the value is compared with so far measured maximum and minimum values, eventually

stored as one. This is just an ordinary search for maximum and minimum. For time-saving purposes, if the maximum value has been already measured and at least three measurements proceed, the program quits the loop. If not, the motor is turned one step further. The loop quits eventually if the whole matrix was measured.

After quitting the loop, the direction of dependence *direction* is determined and stored, because with rise of angle the power either decreases or increases (further explanation in Section 2.3, Fig.6 and below). Also the working point is evaluated.

Next scan is done in order to measure the proximity of working point, so that the program should know how to regulate. The size of the scanned area is given relatively from the working angle by the constants defining its upper border for power increase and lower border for power decrease. In our case,  $upper\_border = 7^\circ$ ,  $lower\_border = 3^\circ$ . The regulation dependence is saved to global variable  $reg\_tab$  (regulation table), which is array of structures. The individual structure contains angle position and appropriate power value. The size of this array is evaluated from

$$size(reg\_tab) = \frac{lower\_border + upper\_border}{step}, \quad (17)$$

where  $step$  variable is step of the scan in degrees. In our case,  $step = 0.2^\circ$ .

Because the scanning of this dependence is essential for stabilization, the range and step must be set accordingly to provide good performance. It must be considered, that the scanning takes some time and the power we are trying to stabilize is fluctuating. Either the measurement should be as fast as possible or the regulation curve for the particular regulator (half-wave plate) should be measured using very stable source and stored for example to file. However, in our case the program and setup is meant to be universal and to stabilize long-time distortions, so the first solution is chosen.

First, the motor is set to the upper border, because it is closer from the last motor position (due to the design of the first scan, the last motor position is most likely near the transmission maximum). The loop starts by measuring the power value two times and then their mean value is saved to regulation table. This has to be done in order to diminish the effect of fluctuations on the measured regulation dependence. The actual motor position is saved to the regulation table together with power,. Motor is then moved by step towards the lower border. The loop ends while the whole regulation table was measured. After that, the motor is set to the working point.

## 4.5 Stabilization loop

This function is essential to the stabilization process itself. It begins with setting the desired sustained power value  $stab\_pwr$ , which is chosen to be the power value of the working angle set in the regulation table. Also the initial table position and other initial variables are set.

Regulation loop is infinite, because we do not need to quit the stabilization in other way than by terminating the program. It starts by acquiring the power value  $act\_pwr$ . If the power value seems to be misread (the communication with FieldMaster GS meter lacks any kind of transmission error check and it sends sometimes a flaw value with +/- 1e-06 error for unknown reason) or if the fast peak of power is read (our device is unable to stabilize such short bursts), the power value is read again. This is determined by evaluating the absolute difference between actual power read and the desired sustained power value and comparing the result with fixed number, which is determined empirically. In our case the program evaluates inequation

$$|act\_pwr - stab\_pwr| > 0.08e-05, \quad (18)$$

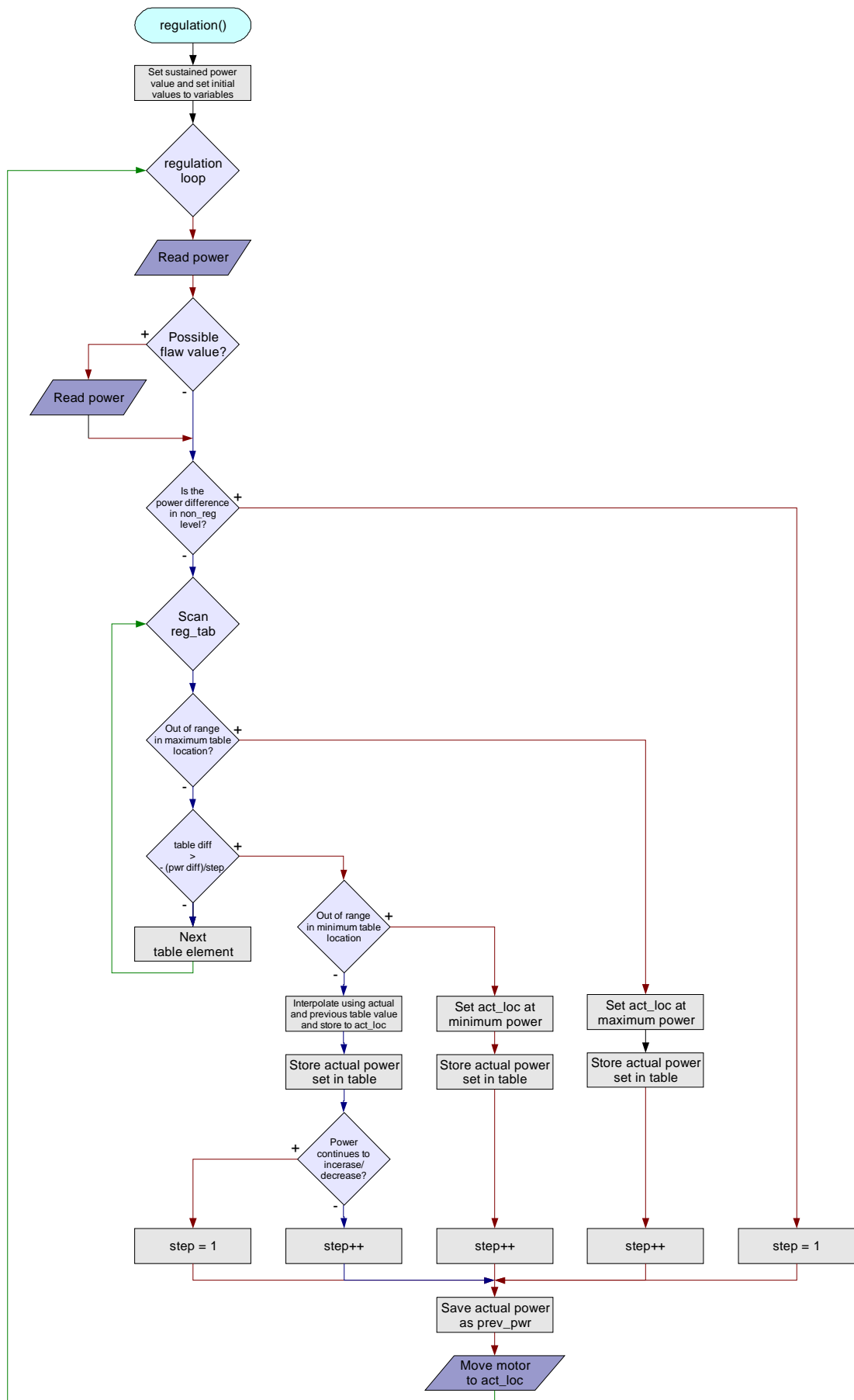
Speed of stabilization is slowed down a little bit, but if we did not insert this condition, the stabilization will suffer from occasional oscillations due to errors in power reading.

After the power is read, the acquired power value is tested to be in the non regulation level. This is done according to inequation

$$|act\_pwr - stab\_pwr| < non\_reg\_level \cdot stab\_pwr, \quad (19)$$

where  $non\_reg\_level$  is the non regulation level constant. If the inequation is true, then the program leaves the position of motor as it is.

For the best performance of the stabilization it is important to set the  $non\_reg\_level$  which means the percentage of  $stab\_pwr$  value in which the stabilization device will not cause any action to stabilized output. It has to be done, because stabilization device isn't able to stabilize short-time fluctuations and without this setting it will create additional noise. Magnitude of this level depends on particular stabilized source. Result of the different  $non\_reg\_level$  setting can be seen in Fig.9. We empirically determined  $non\_reg\_level$  value to be 0.0008 (0.08% of stabilized power) for OZ OPTICS diode laser and 0.0011 (0.11% of stabilized power) for MIRA laser.



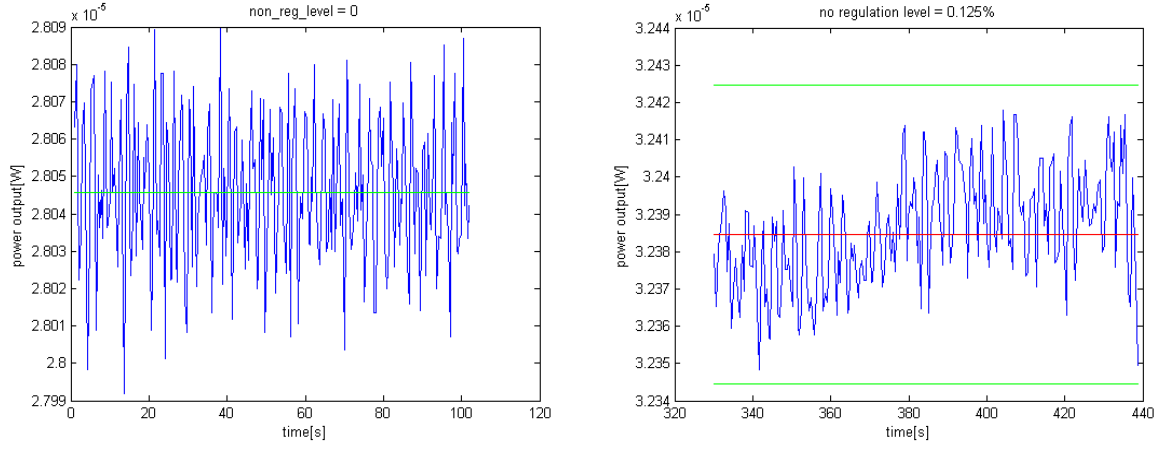


Figure 9: Different *non\_reg\_level* settings for OZ OPTICS diode laser. The red line indicates the sustained power value and green lines are the boundaries of the no regulation area. If *non\_reg\_level* is set to 0%, then the regulator adds unnecessary noise to the output. On the opposite, if *non\_reg\_level* is set to 0.125%, then the regulation didn't take place and the power oscillates between no regulation area borders.

The program continues in going through the regulation table. The purpose is to find an appropriate response in regulation table to actual power deviation from sustained power value *stab\_pwr*. First thing in the loop is to check if we run with table index out of maximum range. If we do, there are two options considered, either to extrapolate the regulation table dependence to desired point or to simply set the maximal power output. The second possibility was chosen, because we generally won't deal with fluctuations that big and because the speed of motor is very slow and it will take a long time to move the motor to compensate such power deviation. However, the program version with extrapolation was also created.

Next statement is essential for the cycle. It checks the variable table position according to inequation

$$reg\_tab[i].power - set\_tbl\_pwr > -\frac{act\_pwr - stab\_pwr}{step}, \quad (20)$$

the *reg\_tab[i].power* stands for the power selected by cycle; *set\_tbl\_pwr* is the table power corresponding to actual motor position. The cycle runs variable *i* in the way that the value in *reg\_tab[i].power* is increasing. The inequation compares the changing table power difference with the negative power difference on the power output divided by variable *step*, explained below.

If the statement (20) gets to be true, it means that the response to the measured power fluctuation should be found in regulation table in the position between (i-1)<sup>th</sup> and i<sup>th</sup> items. At first the program checks if the variable *i* isn't 0 (that means the table minimum), if it is then the table is either extrapolated or the minimum output is set. We choose the second solution, simi-

larly as in previous case of getting out of table maximum. Generally, when the statement (20) is true, it doesn't mean that the actual response is the table value (this is further discussed in chapter 2.3). For the higher accuracy the program linearly interpolates the needed response position value from (i-1)<sup>th</sup> and i<sup>th</sup> table item using the equation

$$act\_loc = reg\_tab[i].loc - diff\_pwr \cdot \frac{reg\_tab[i].loc - reg\_tab[i-1].loc}{reg\_tab[i].power - reg\_tab[i-1].power}, \quad (21)$$

where the *diff\_pwr* is the table quantization step.

$$diff\_pwr = (reg\_tab[i].power - set\_tbl\_pwr) - \left( - \frac{act\_pwr - stab\_pwr}{step} \right). \quad (22)$$

This causes the regulation to act very quickly to the power fluctuations; stabilized power level is often achieved in 1 or 2 stabilization steps.

The variable *step* in (20) is important, because it prevents stabilization procedure from oscillating (mentioned in Section 2.1). It works like this: If the measured power continues to increase or decrease, the value of the *step* is set to 1. Otherwise, if the power decreases after the previous increase and vice versa, the *step* value is increased, so the response is lower than the actual fluctuation. This solution prevents the regulation from oscillation, because the eventual resonant feedback response is diminished quickly to minimum. Also the existence of the non regulation level helps in this case, but the oscillation prevention works even with the *non\_reg\_level* set to zero.

After the response is calculated, table power corresponding to the response position *act\_loc* is stored to *set\_tbl\_pwr*, although this doesn't mean that the power value is one of the table values. Corresponding table power value is saved according to equation

$$set\_tbl\_pwr = reg\_tab[i].power - diff\_pwr. \quad (23)$$

Then it is determined, if the power continued to increase/decrease and the variable *step* is set accordingly.

Now the program has found the proper response to deviation, so the actual power in *act\_pwr* is stored to variable *prev\_pwr* and finally the motor is given the command to move to *act\_loc* to compensate the power change.

## 5 Stabilization performance

A stabilization device is characterized by a time delay between two reactions. The presented device is characterized by the minimum delay between detection of variation in the input signal and the response  $T_{min} = (187.9 \pm 0.3)$  ms. This time delay is caused mainly by the long waiting time of the data transfer from meter. The empiric value of communication timeout with meter is 90ms. The average delay  $T_{avg}$  depends on the size of the compensation step, on the setting of *non\_reg\_level* variable and on the particular stabilization. This delay is additionally caused by the motor reaction and the motor controller transfer delay. The empiric value of communication timeout with motor is 30ms. The average regulation delay will be evaluated individually for each output as a mean value of response times in one hour of measured data. The value of no regulation level roughly determines the size of the stabilized output fluctuations.

### 5.1 Continuous-wave diode laser

We applied the presented device to stabilize a diode laser (OZ OPTICS). The unstabilized power time evolution of this laser was measured and it is shown in Fig.2. The effect of stabilization of the power output of the laser and Allan variance of power time evolution is shown in Fig.10. The sustained power value is  $P_{sust} = 31.51 \mu W$ , that is 76.3% of maximum power. No regulation level is set to 0.08% of  $P_{sust}$ . In each of the following graphs of power evolution the approximately 6% of total power is measured by detector DET (Fig. 8).

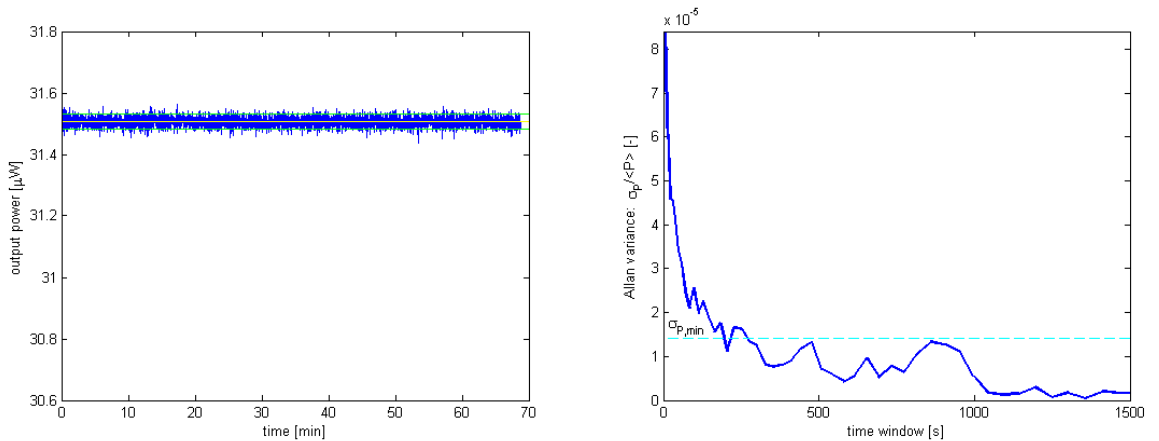


Figure 10: Stabilized OZ OPTICS diode laser source power output and its Allan variance. The green lines specify the no regulation interval. The horizontal line at  $\sigma_{P,\min} = 1,4 \times 10^{-5}$  represents the minimum AVAR value of the unstabilized source (compare with Fig.3).

When comparing Fig.2, Fig. 3 and Fig.10 we can say that the stabilization proceeds successfully within the time range we are interested in. In the short times the stabilization device

adds a small amount of noise to the power output. For longer times the AVAR of the stabilized source is always smaller than the minimum AVAR of the unstabilized source. The average regulation delay was measured to be  $T_{avg} = (220 \pm 70)$  ms.

## 5.2 DPSS laser in pulse regime

We stabilized the output of MIRA 900 laser at 800 nm in pulse regime with repetition rate 76 MHz. MIRA was started approximately 7 hours before the measurement. The sustained power value is  $P_{sust} = 89.26 \mu\text{W}$  that is 79% of maximum power. The no-regulation level is set to 0.11% of  $P_{sust}$ . The average regulation delay was measured to be  $T_{avg} = (250 \pm 110)$  ms.

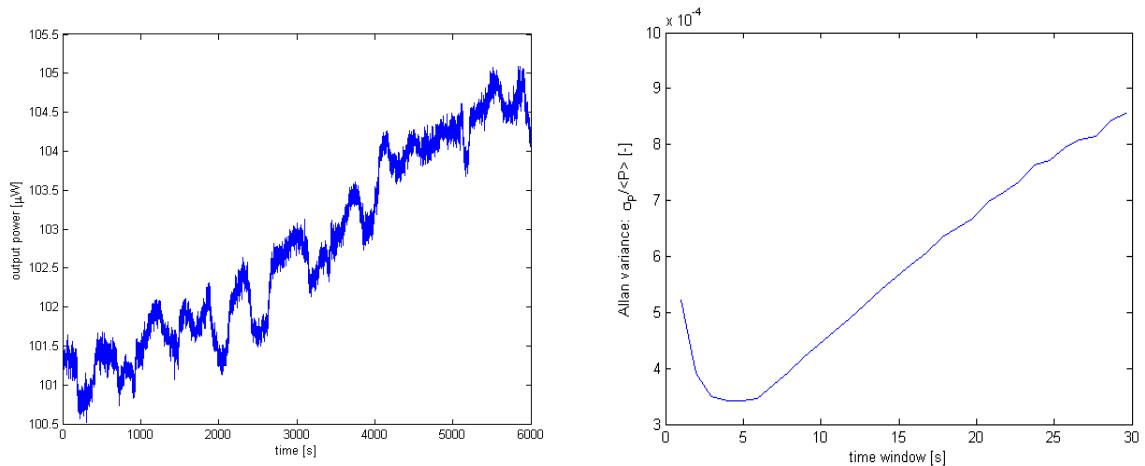


Figure 11: Unstabilized output of MIRA 900 laser in pulse mode and its AVAR. The power drift is about 3.3% per hour. The AVAR reaches its minimum value  $\sigma_{P,\min} = 34 \times 10^{-5}$  for  $\tau = 4$  s.

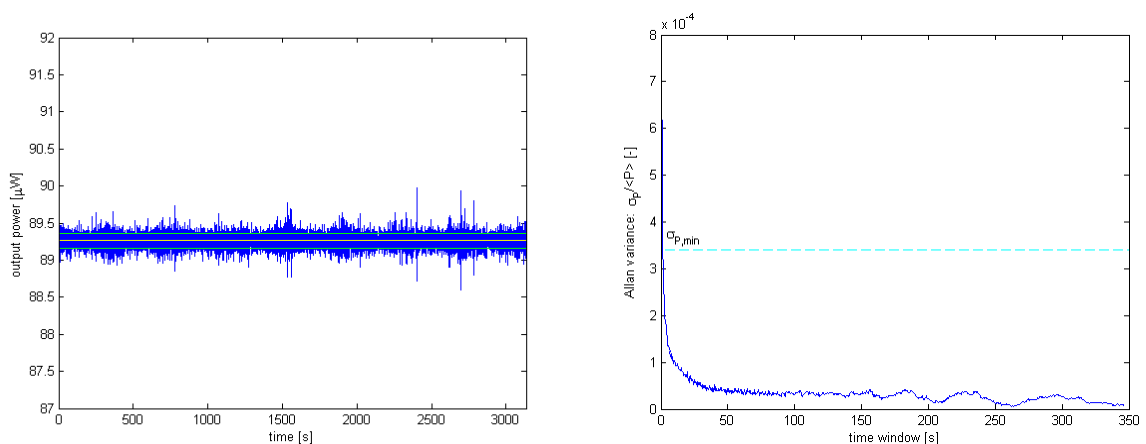


Figure 12: Stabilized output of MIRA 900 laser in pulse regime and its AVAR. The green lines specify the no regulation interval.

### 5.3 DPSS laser in pulse regime with temperature variations

The laser MIRA 900 in the same regime as in chapter 5.2 was stabilized. The temperature in the laboratory was lowered by 3 degrees prior to the first measurement start. The laser was running approx. 5 hours before the measurement. The sustained power is  $P_{sust} = 255 \mu\text{W}$ , that is 84.7% of maximum power. The no-regulation level is set to 0.13% of sustained power. The average regulation delay was measured to be  $T_{avg} = (580 \pm 250) \text{ ms}$ . This is caused mainly by large fluctuations of source and it results in much longer motor movement to compensate.

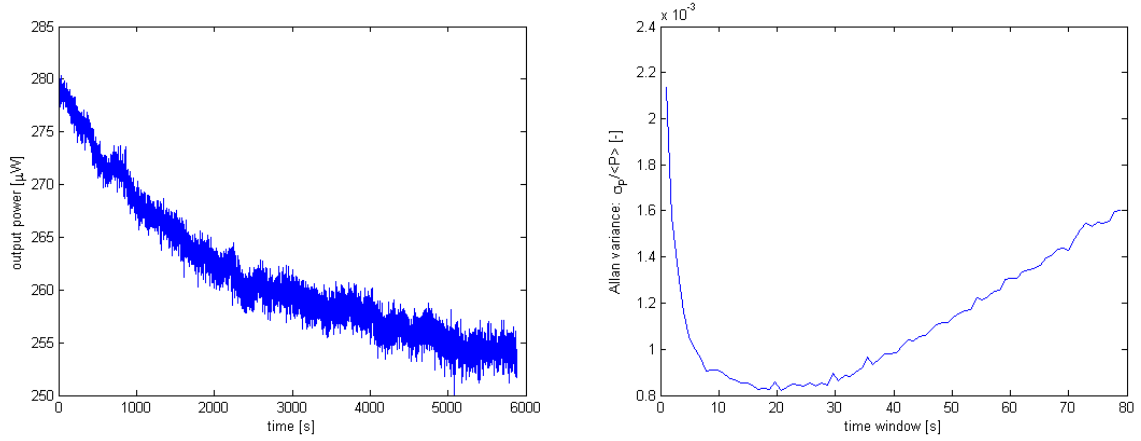


Figure 13: Unstabilized output of MIRA 900 laser and its AVAR. The power drift is about 7.3% per hour. The minimum AVAR value  $\sigma_{P,\min} = 82 \times 10^{-5}$  is at  $\tau = 20.7 \text{ s}$ .

The output power of laser in environment with changing temperature tends more to fluctuate. The fluctuations increased in both short and long times, see Fig.13. Although the time of AVAR minimum raised from  $\tau = 4 \text{ s}$  for normal environment to  $\tau = 20.7 \text{ s}$  for environment with varying temperature, the minimum AVAR value increased from  $\sigma_{P,\min} = 34 \times 10^{-5}$  to  $\sigma_{P,\min} = 82 \cdot 10^{-5}$ , respectively. This means that the relative size of fluctuations increased more than 2 times.

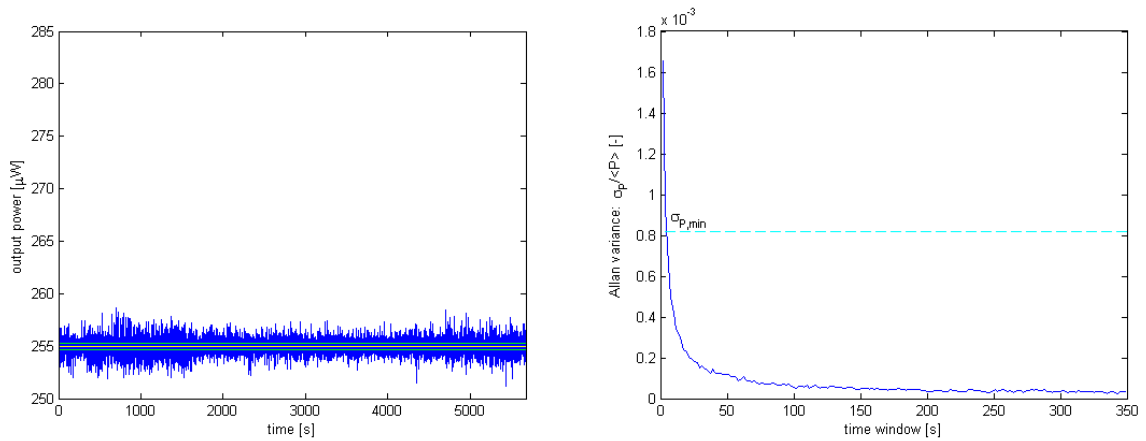


Figure 14: Stabilized output of MIRA 900 laser and its AVAR.

## 6 Possible improvement

The problematic serial communication with FieldMaster power meter and the long time delay in communication was discussed in Chapters 4 and 5. Further, the motor and meter needs to be connected to and controlled by a personal computer. The stabilization program is far from using all the computer performance and it occupies the computer which can be used to another purposes.

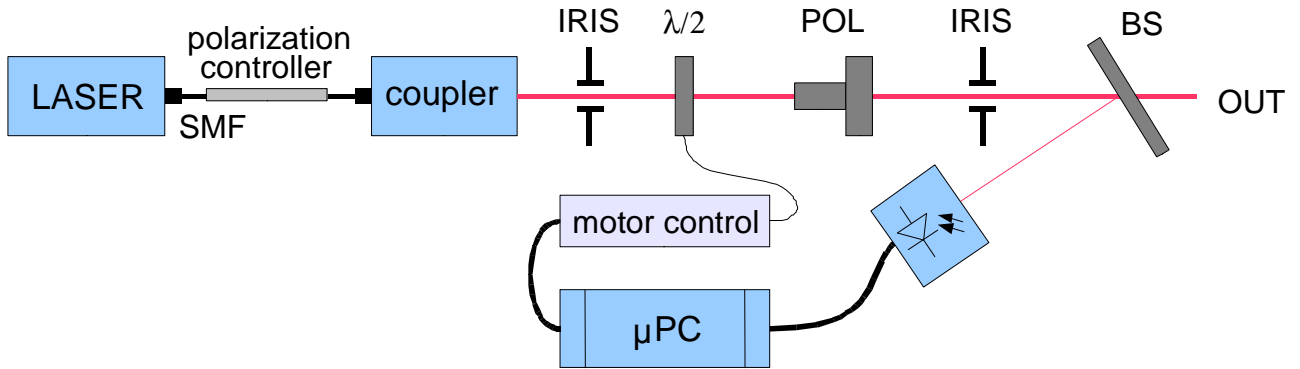


Figure 15: Stabilization device controlled by microchip. The Si PIN photodiode S3883 (Hamamatsu) is used as a detector.

The idea is to replace the FieldMaster power meter (detector) and eventually both the detector and the computer (detector + regulator) with an electronic circuit controlled by a microcontroller (Fig. 15). The layout of the designed circuit is shown in Appendix A. The microcontroller PIC18F1230 (Microchip) is chosen. PIC18F1230 is equipped with USART module. The USART provides resources to communicate with other RS-232 devices; these are the personal computer and eventually motor controller. Further, PIC18F1230 contains 10-bit A/D converter, which is used to convert the signal from S3883 PIN photodiode (Hamamatsu) to a digital representation. Additionally, the 8kB flash memory of PIC18F1230 is sufficient for storing the code of the stabilization program. More information can be found in manufacturer's datasheet [5].

The S3883 PIN photodiode current must be converted to voltage and amplified prior to entering the microcontroller's A/D converter. There we use the transimpedance amplifier previously assembled in the laboratory (see Appendix B for the schematic of the amplifier).

The developed microcontroller circuit is shown in Appendix C. The circuit can work either as a detector with computer connected to RS-232 on board or as a detector and a regulator connected to motor controller. The difference is only in the microcontroller control software.

The circuit was designed and mounted and basic control software was written, but in the time of writing this thesis it is not properly tested.

## 7 Conclusion

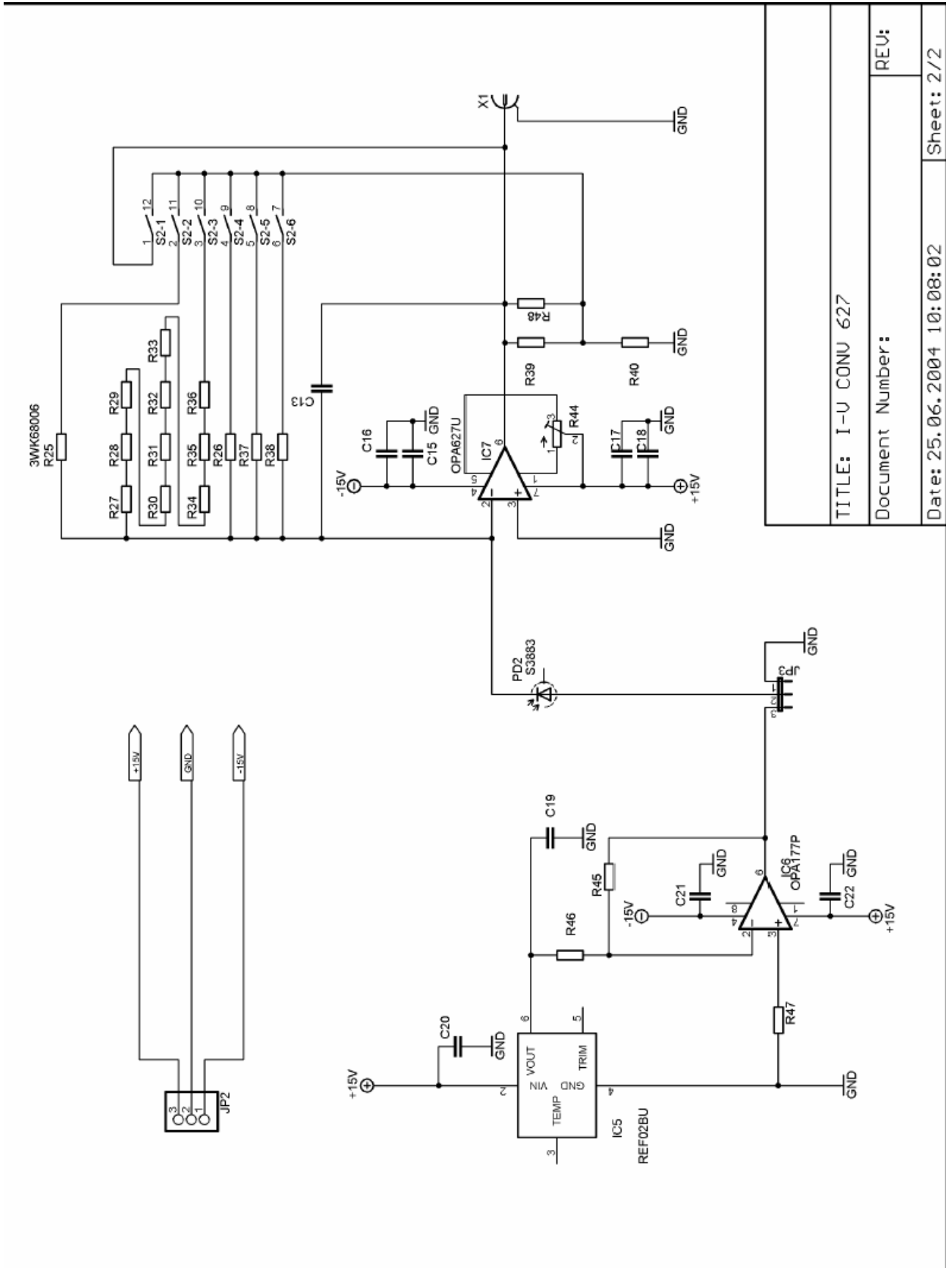
The working stabilization device is presented in this thesis. The performance of the stabilization is sufficient for stabilizing all tested laser sources. The minimal response time that the device needs to regulate the power output is  $T_{min} = (187.9 \pm 0.3)$  ms. The stabilization is effective in the range of seconds and more. The typical use of the developed device is to stabilize laser sources for the optical experiments. Occasional oscillations of the stabilization are successfully reduced by a control algorithm and the magnitude of oscillations is in the range of unstabilized noise.

The Allan variance is presented as a powerful tool for characterizing both the magnitude and the optimal measurement time of the optical power noise. The optical power stability improvement caused by the stabilization can be described by comparing the minimum Allan variance in the required time window (e.g. the mean time of measurement in the experiment). For the demonstrating purposes we take the time scale of 30 s. The output of DPSS laser measured in Section 5.2 improved from relative Allan variance value  $86 \times 10^{-5}$  for unstabilized source to value  $4.8 \times 10^{-5}$  for stabilized source. The average size of fluctuations in the time range of 30 s was reduced 18 times. The measured results confirm the feasibility of Allan variance for describing the signal noise and mean level drift.

The proposed scheme can be improved by replacing the FieldMaster GS power meter and eventually the personal computer with microcontroller circuit which results in much shorter response time  $T_{min}$ .



# Appendix B: PIN voltage amplifier schematic

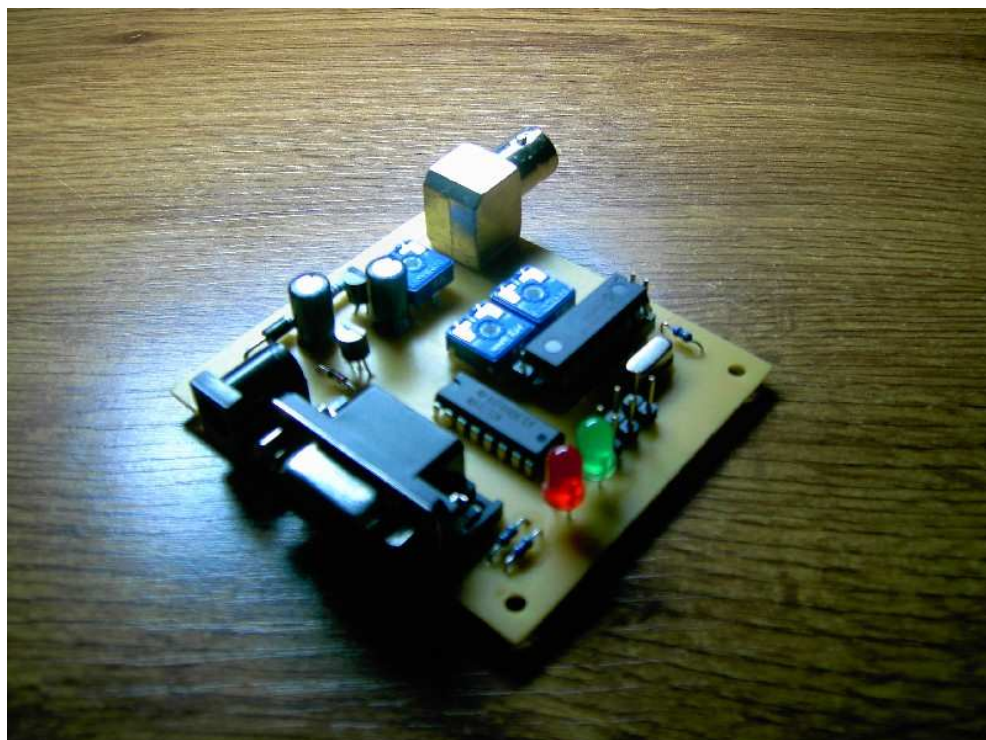
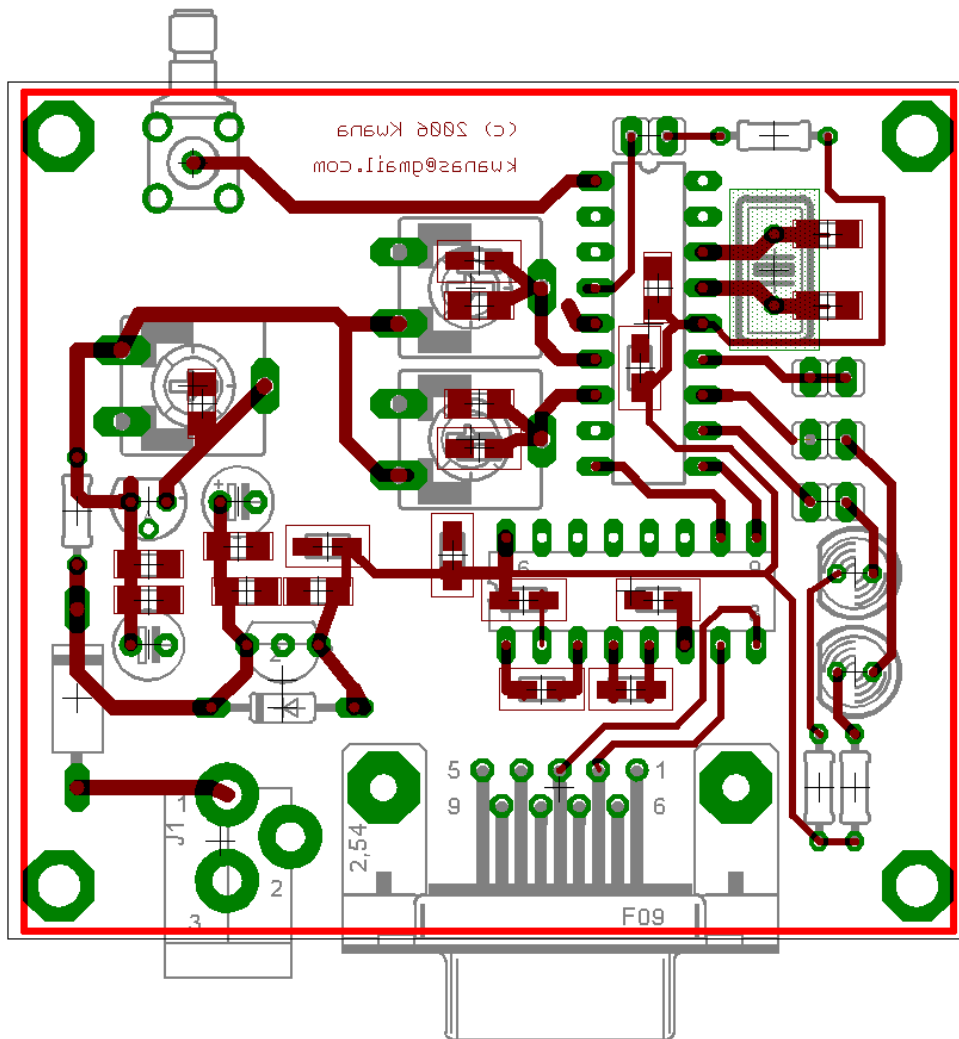


TITLE: I-U CONU 627

Document Number: REV:

Date: 25.06.2004 10:08:02 Sheet: 2/2

## Appendix C: Layout of the mounted microcontroller board



## References

- [1] D. W. Allan, N. Ashby, C. C. Hodge, *The Science of Timekeeping*, Hewlett Packard Application Note 1289, Appendix A and B (1997).
- [2] R. Schieder, C. Kramer, *Optimization of heterodyne observations using Allan variance measurements*, *Astronomy & Astrophysics* 373 (2001).
- [3] L. Slodička, Bachelor thesis *Realization of spatial modes filtration by single-mode optical fiber*, PřF UP, Olomouc (2006).
- [4] B. E.A. Saleh, M. C. Teich, *Fundamentals of Photonics*, John Wiley & Sons Inc. (1991).
- [5] Microchip Technology Inc., *PIC18F1220/1320 Data Sheet* (2007).
- [6] M. R. Sweet, *Serial Programming Guide for POSIX Operating Systems*, GNU FDL 5th Edition, 6th Revision (2005).
- [7] Various authors, *man - Linux Manual pages*.
- [8] L. Conti, M. de Rosa, F. Marin, *Low-amplitude-noise laser for AURIGA detector optical readout*, *Applied Optics* Vol. 39, No. 31 (2000).
- [9] J. Fischer, L. Fu, *Photodiode nonlinearity measurement with an intensity stabilized laser as a radiation source*, *Applied Optics* Vol. 32, No. 22 (1993).